Digestive System Membranes: Freeze-fracture Evidence for Differentiation and Flow in *Paramecium*

RICHARD D. ALLEN and L. A. STAEHELIN
Pacific Biomedical Research Center and Department of Microbiology, University of Hawaii, Honolulu, Hawaii 96822, and Department of Molecular, Cellular and Developmental Biology, University of Colorado, Boulder, Colorado 80302

ABSTRACT Freeze-fractured membranes of digestive vacuoles of randomly feeding *Paramecium caudatum* exhibit dramatic differences in intramembrane particle (IMP) number and distribution on both E- and P-fracture faces. By pulse-feeding latex spheres to cells we have demonstrated that these differences are related to the age of the digestive vacuoles, and that the membranes of such vacuoles undergo a specific sequence of changes during the digestive cycle. Young digestive vacuoles (DV-I; ≤6 min), nascent vacuoles still connected to the cytopharynx, and discoidal vesicles, from which vacuole membrane is derived, all have a highly particulate E face and a less particulate P face. As early as 3 min after feeding, a second category of digestive vacuoles (DV-II) can be recognized, which are both considerably smaller in diameter and lack particles on their E face. These findings suggest that the endocytic removal of DV-I membrane material associated with the formation of DV-II vacuoles involves a concomitant and selective removal of E-face particles, as essentially no changes are seen in the density of P-face particles on the two types of vacuoles. Beginning at 10 min the first DV-III vacuoles are encountered. These are both larger than the DV-II vacuoles and possess very prominent E-face particles, which resemble those on the E face of the numerous lysosomes bordering the digestive vacuoles. DV-III vacuoles also exhibit a substantial increase in P-face particles. These membrane changes closely parallel, and are probably correlated with, the physiological events occurring within the vacuole lumen: concentration of food, killing of prey, and digestion. Calculations of the amount of membrane removed from DV-I to form DV-II and of the increase in membrane surface area during the transition from DV-II to DV-III indicate that as much as 90% of the initial phagosome (DV-I) membrane can be removed before digestion begins. The enlargement of DV-II must be caused by fusion with adjacent lysosomes which also contribute the new populations of IMPs to the DV-III membrane. The appearance of numerous endocytic structures on older DV-III vacuoles suggests that membrane is retrieved from DV-III before defecation.

Intramembrane particles (IMPs) within digestive vacuole membrane of protozoa are known to vary both in number and in their distribution relative to the two fracture faces of the membrane and with vacuole age. IMP changes have been observed in phagosomes of *Acanthamoeba castellanii* (10), in *Tetrahymena pyriformis* (9, 13), and also in *Paramecium caudatum* (2, 4). These IMP changes indicate that membranes surrounding the foci of digestion are not static, impassive boundaries simply separating the digestive events from the cells other metabolic activities, but are themselves involved in a dynamic way in at least some of the events that they are partitioning.

The fact that the digestive vacuole membrane can undergo compositional changes raises a number of questions. Where do new IMPs come from when the IMP number increases and where do they go when the IMP number decreases? Why do

THE JOURNAL OF CELL BIOLOGY · VOLUME 89 APRIL 1981 9-20

some stages of digestive vacuole membranes have more IMPs on the E rather than P face when they are fractured while others have the reverse? And, of utmost importance, what is the functional role of the various sizes of IMPs in the membranes?

In this study we have extended previous freeze-fracture observations (2) on *P. caudatum* by employing a timed study of the changes that occur in the digestive vacuole membranes from the initiation of vacuole formation to the time the vacuoles are 60 min old. We have also followed in this study two other membrane pools that become part of the digestive vacuole membrane at specific times in the digestion cycle. These are the discoidal vesicles, a pool of membrane from which the initial vacuole membrane is derived (1), and the "secondary" lysosomes, which may be identical to the "neutral red granules" observed by light microscopists (18).

Our freeze-fracture replicas show dramatic and consistent changes in the membranes of the digestive vacuoles that are intimately correlated in time with the condensation and the killing of the contained food organisms. We also demonstate the acquisition of a new population of IMPs during the time the phagosome becomes a phagolysosome, which is during vacuole growth, a time that coincides with the beginning of digestion. These latter vacuoles have a membrane similar to those of lysosomes that surrounds these early digestive vacuoles. On the basis of the changes in IMPs in the membranes and the endocytic and exocytic events that occur during the digestive cycle, as well as theoretical determinations of the quantity of membranes involved, we elaborate on and provide further evidence for the probable course of membrane flow in the digestive system of this cell.

Preliminary reports of this work have been published (3, 4) and some of the data have been included in a review (6).

MATERIALS AND METHODS

Handling Cells

Paramecium caudatum was grown at room temperature on bacterized Cerophyl medium which also contained boiled wheat grains. Cells were concentrated from cultures that had reached a high population (stationary phase) by centrifugation in a clinical centrifuge. To 0.5 ml of lightly packed cells was added 6.5 ml of 0.5% glutaraldehyde buffered in 0.05 M cacodylate at pH 7.4. Fixation was carried out for 15 min at room temperature. The fixed cells were washed in buffer and then placed in 25–30% glycerol for 2 h. These glycerinated cells were then used for subsequent freeze-fracturing.

Pulse-chase Studies with Latex Spheres

To determine the age of individual digestive vacuoles in the freeze-fracture replicas, we fed the cells polystyrene, monodisperse latex beads of 0.091 μm diameter in a series of pulse-chase experiments. The latex beads were obtained from Polysciences, Inc. (Warrington, Pa.) and were used directly from the dropper bottle by adding one drop to 2 ml of concentrated cells. The cells remained in the presence of latex for 3 min. They were spun down during the 3rd min and the latex-containing medium was decanted precisely at 3 min; the cells were then washed in two changes of fresh Cerophyl growth medium when experiments required a chase. Where no chase was used, cells were fixed after 30 s, 60 s, 90 s, and 3 min directly in the latex-containing medium. Cells chased in fresh medium were fixed after intervals of 6, 10, 20, 30, 50, and 60 min. In these cells the age of any vacuoles containing appreciable quantities of latex could be determined to within a 3-min interval of time.

Freeze-fracturing

After fixation and washing in cacodylate buffer the cells were frozen in Freon 12 and transferred to liquid nitrogen. Fractures were made at −106°C in a Balzers BA 360 freeze-etch unit (Balzers High Vacuum Corp., Santa Ana, Calif.). The fractured surface was shadowed at a 45° angle with an electron gun at 1,900 V using platinum-carbon; carbon was then evaporated at a 90° angle. The replicas were cleaned 1–3 h in bleach followed by 20% chromic acid overnight and an additional hour in 40% chromic acid the following day. To dissolve the contaminating latex spheres the replicas were also washed for 1 h in tetrahydrofuran (23) before a final wash in double-distilled water. Replicas were picked up on Formvar-coated one-hole grids.

Calculation of Structural Membrane Parameters

Replicas were viewed in a JEM-100B or Hitachi HU-11A electron microscope. Only those digestive vacuoles that were fractured so as to expose both the membrane and some of the lumen, containing latex beads, were used for further evaluation. All micrographs for particle anaysis were taken at × 31,000 and then enlarged to × 200,000 for counting and measuring IMPs. IMPs in a sufficient number of 0.01-μm^2 squares were counted so that an area of at least 1 μm^2 on both the E- and P-fracture faces of each of five different membrane populations was obtained. Where particle numbers were low, up to 4-μm^2 membrane area was counted. No correction was made for possible effects on the counts of tilting of membranes in the replicas. However, whenever possible, the areas were chosen to minimize this error. The great heterogeneity of particles in terms of their size and height does not always allow easy identification of particles, particularly where they are tightly packed. Thus, the total counts can be considered only approximations of the real particle numbers.

Counts were obtained from 5 to 13 different vacuoles for each different membrane fracture face. IMPs from a much larger number of discoidal vesicles and lysosomes were counted. Particle sizes were measured by the method of Staehelin (22). However, because of the small number of particles on some types of vacuoles, and the difficulty in obtaining suitable images of others, adequate numbers of particles for quantitative analysis were very difficult to obtain in some instances.

The dimensions of vacuoles, lysosomes, and endosomes were determined from the electron micrographs of the replicas.

RESULTS

Size and Stage Classification of Digestive Vacuoles

As reported by light microscopists (14), the newly formed digestive vacuole is relatively large; it then condenses, after which it again grows in size. In our replicas the largest labeled vacuole in samples collected between 30 s and 3 min after addition of the latex to the medium had a diameter of 14.3 μm. Shortly thereafter, the labeled vacuoles are similar in diameter. These small vacuoles are quite spherical in shape and contain a tightly packed content of bacteria and latex spheres. No sign of digestion was detectable at this time. The ultimate condensation seems to be partially determined by the particulate content of the vacuole. The membrane surface area is frequently reduced until the particle clump cannot be further compacted. Vacuoles at this stage were as small as 3.5 μm in diameter. After condensation, the vacuoles again grow in size. Their membrane topography becomes wavy as opposed to the smooth spherical shape of the preceding stage. Vacuoles now

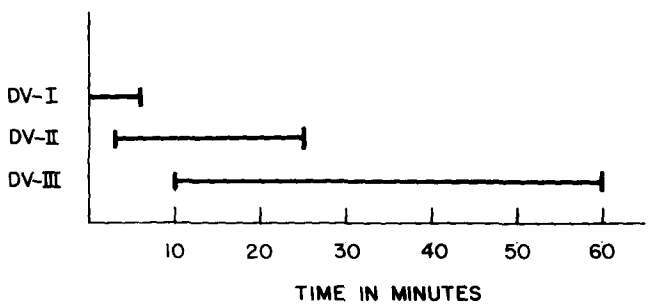

FIGURE 1 Digestive vacuoles (DV) can be divided into three stages according to their IMP number and distribution. The times of the first and last appearance of each stage in our fractures are indicated by the ends of the lines.

have a characteristic IMP pattern (to be described below) as do each of the first two stages. Latex spheres and bacteria are no longer clumped but are dispersed within these vacuoles. Signs of digestion, the appearance of membrane whorls, are now evident. The diameters of the expanded vacuoles vary but are up to 16.4 μm in the replicas.

The distinctiveness of each of these three populations of vacuoles led us to separate digestive vacuoles (DVs) into three

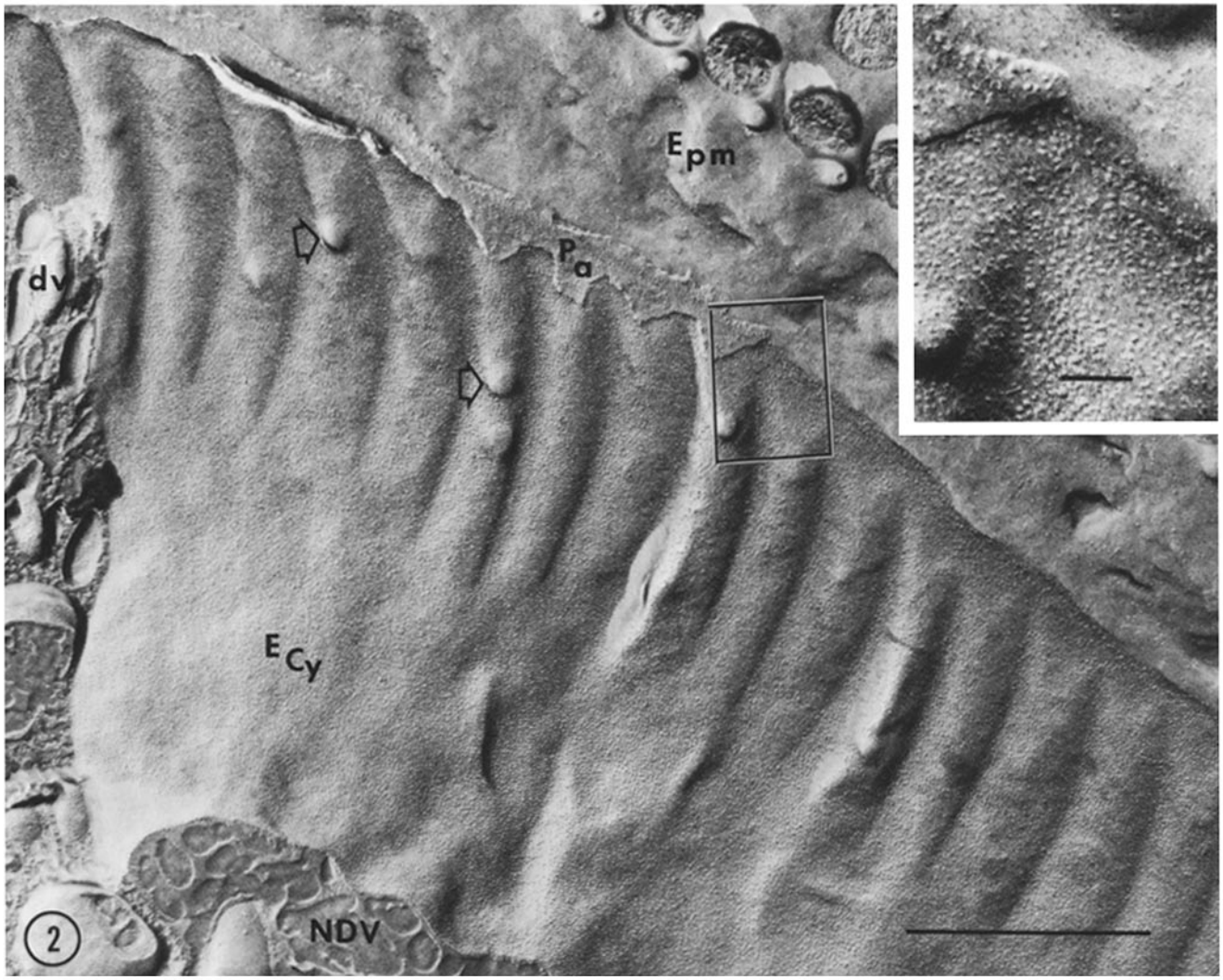

FIGURE 2 E face of the cytopharyngeal membrane (E_{Cy}) showing its high density of IMPs and in contrast the low number of IMPs on the plasma membrane of the buccal cavity (E_{pm}) with which it is continuous (see also inset of area in box). A fragment of the alveolar membrane with its P face exposed (P_a) remains along the intracellular junction which joins the alveolus to the cytopharyngeal membrane. Pockets on the cytopharynx (arrows) probably indicate partially incorporated discoidal vesicles. *NDV*, lumen of nascent digestive vacuole; *dv*, discoidal vesicles in cytoplasm. Bar, 1 μm; *inset*, 0.1 μm. × 35,000; *inset*, × 100,000.

FIGURE 3 The E face of the cytopharyngeal membrane has 4,574 ± 733 IMPs/μm^2. × 100,000.

FIGURE 4 The P face of the cytopharyngeal membrane has 1,142 ± 365 IMPs/μm^2. Bar, 0.1 μm. × 100,000.

groups on the basis of their age, size, membrane topography, and IMP patterns. Each population will be considered separately and will be referred to as DV-I: nascent and condensing vacuoles; DV-II: condensed vacuoles; and DV-III: expanding and mature vacuoles. DV-I were determined by labeling to be from 0- to 6-min old, DV-II from 3- to 25-min old, and DV-III 10- to 60-min or more in age (Fig. 1). Although considerable overlap in age existed between the different stages, the population to which a particular vacuole should be placed was usually apparent based on the above parameters. Transition stages also existed and probably accounted for those vacuoles that could not be easily classified into one of the three stages.

Membrane Fracture Faces of the Cytopharynx and Stage I Digestive Vacuoles (DV-I)

DVs arise from the cytopharynx. The membrane of the cytopharynx expands as discoidal vesicles fuse with the left margin of the cytopharyngeal area of *Paramecium* (1). In fractures the cytopharyngeal membrane is seen to be continuous with the plasma membrane of the buccal cavity (Fig. 2). However, this membrane is dramatically different from the plasma membrane both in IMP numbers and in IMP distribution (Fig. 2, *inset*). The transition between the plasma membrane and the cytopharynx membrane is very sharp (Fig. 2) and corresponds to the pericellular intermembranous junction between the plasma membrane and the margin of the underlying flattened cisternae of the alveoli (5). The face of the cytopharyngeal membrane is covered with particles (Fig. 3), while the P face has only a few particles but numerous pits, which give it a rough appearance (Fig. 4). The ridges of the cytopharyngeal membrane, formed by the folding of this membrane over the cytopharyngeal microtubular ribbons (1), contain membrane pockets (arrows, Fig. 2) which are most likely caused by discoidal vesicle fusion with and partial incorporation into the cytopharyngeal membrane.

DV-I (Fig. 5) have an IMP content and distribution similar to that of the cytopharyngeal membrane. However, most of these vacuoles show extensive membrane blebbing into the cytosol. Fields of tubular and varied-shaped vesicles sometimes accumulate in the space next to these vacuoles (Fig. 5). The diameter of the tubules, 0.1 μm, is approximately the same as that of the fractured necks which are seen on the E face of the fractured vacuole membrane. These tubular vesicles have an IMP number and distribution superficially resembling those of the membrane of the vacuole from which they are derived (Fig. 8).

Some DV-I, particularly those 30 s or less in age, show short invaginations into their lumens. However, no accumulation of vesicles resulting from the pinching off of such luminal invaginations was even seen in the vacuole. It seems that this represents a very early stage in the preparation for endocytic activity of the vacuole membrane, but that actual pinching off takes place only from blebs directed toward the cytosol. Details of early events in membrane remodeling leading to endocytosis are currently being investigated. By 90 s, long tubular blebs that are pinched off appear to be directed toward the cytosol (Figs. 5 and 6).

The numbers of IMPs on the E and P faces of the cytopharynx (Figs. 3 and 4) and DV-I (Figs. 6 and 7) were combined because their respective E faces and P faces were similar. The mean number of IMPs on the E face is 4,575 ± 733 particles/μm^2 while on the P face the number is 1,142 ± 365 particles/μm^2, giving a total of 5,716/μm^2 of membrane surface area (Fig. 9).

Membrane Fracture Faces of Stage II Digestive Vacuoles (DV-II)

The most striking features of the membrane of these condensed DV-II is their extreme change in IMP total number and the almost complete lack of IMPs on the E face (Figs. 10 and 11), which, in the preceding stage, carried such a high number of particles. The E face has only 60 ± 44 particles/μm^2 and many of these were indistinct and open to question. The P face (Fig. 12) carries 1,402 ± 203 IMPs/μm^2 to give a total of 1,462/μm^2.

The topography of the vacuole is generally smooth and there is little or no endocytic activity associated with the membrane (Fig. 10). Vacuoles at this stage are typically surrounded by a large number of lysosomes (Fig. 10).

Membrane Fracture Faces of Stage III Digestive Vacuoles (DV-III)

After stage II (beginning at 10 min), the condensed vacuoles are converted to enlarged DV-III by the acquisition of new membrane material. The topography of these vacuoles is no longer spherical and smooth but is wavy to irregular (Fig. 13). The E face of these vacuoles now bears a population of very prominent IMPs (Fig. 14) probably caused by the unusual height which they project above the leaflet matrix since their average size is only slightly greater than that of the less pronounced P-face particles (Fig. 19). There are 1,144 ± 338 IMP/μm^2 on the E face and 3,367 ± 508/μm^2 on the P face (Fig. 15) for a total of 4,481 IMPs/μm^2, a sharp rise in number from the previous stage.

Some suggestion of endocytic activity is often found in older DV-III (Fig. 16) and the direction of evagination is always into the cytosol. No large accumulation of tubular vesicles as seen near DV-I is found adjacent to these vacuoles. The fractured necks appear to be grouped together in patches rather than

FIGURE 5 A digestive vacuole containing dispersed polystyrene latex spheres (x) indicating it is 90 s or less in age. Its surface shows extensive blebbing and a large field of tubular membrane fragments lies adjacent to the vacuole. Bar, 1 μm. × 20,000.

FIGURE 6 The E face of a digestive vacuole 90 s or less in age. Many fractured necks indicate active blebbing into the cytosol at this age. × 100,000.

FIGURE 7 P face of vacuole 30 s or less in age. *x*, latex bead in the lumen of the vacuole. Bar, 0.1 μm. × 100,000.

FIGURE 8 A higher magnification of the tubular vesicles that are in the cytoplasm next to a DV-I. Cross fractures of such vesicles are circular. E and P faces of these vesicles are morphologically similar in IMPs to discoidal vesicles (compare with Fig. 18). *x*, latex sphere in vacuole lumen. *Cyt*, cytosol; *Vac*, vacuole. Bar, 0.2 μm. × 75,000.

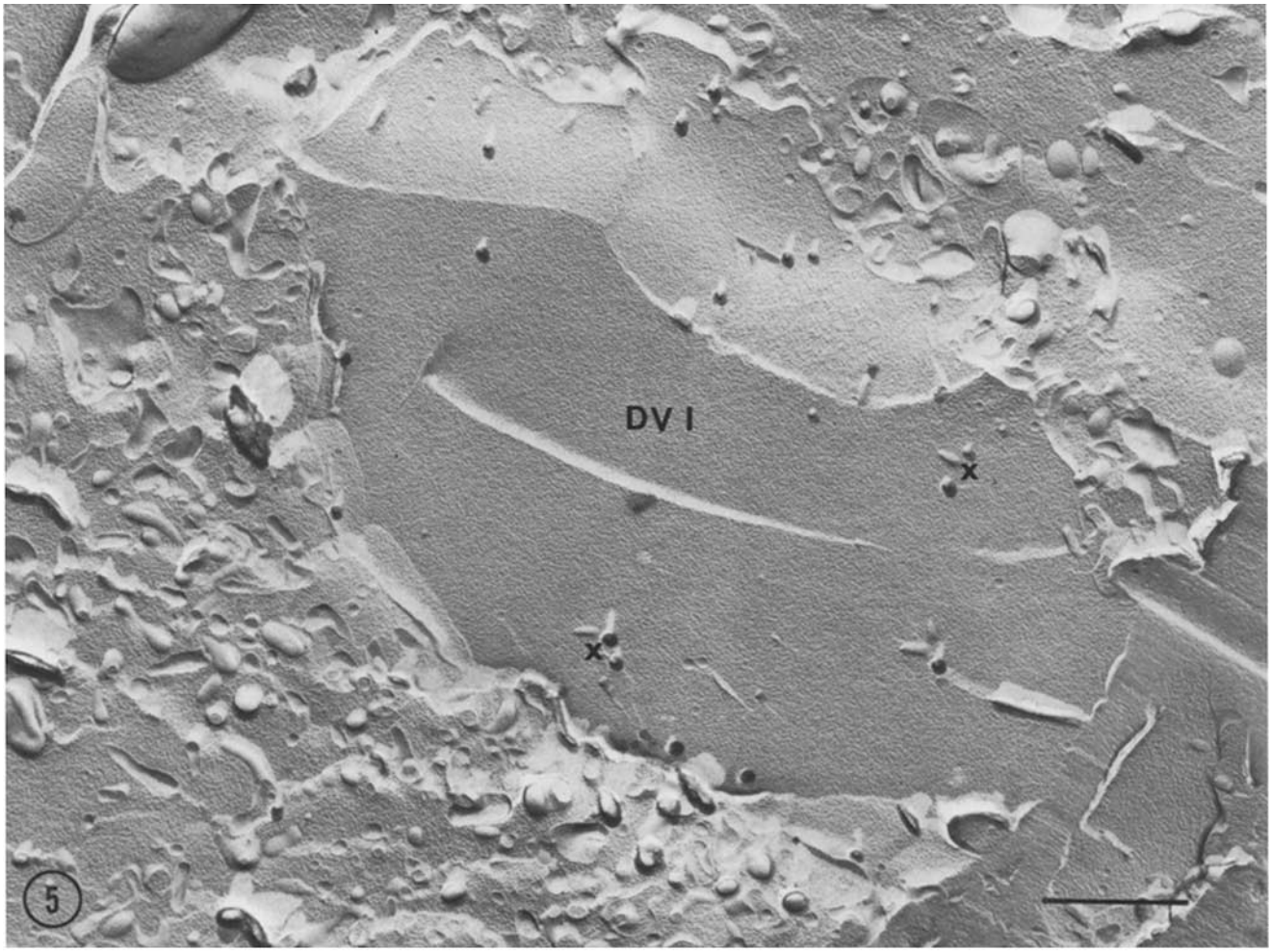
DV I
x
x
5


E I
6

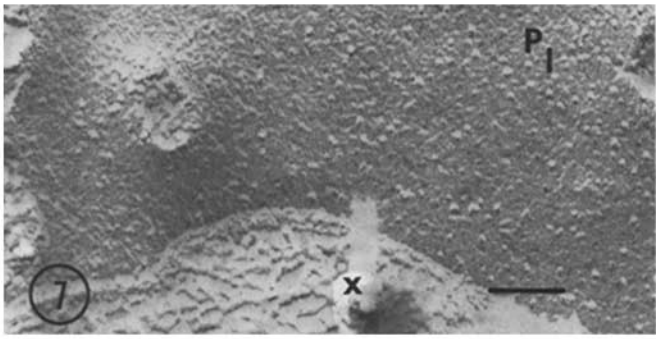
P I
x
7

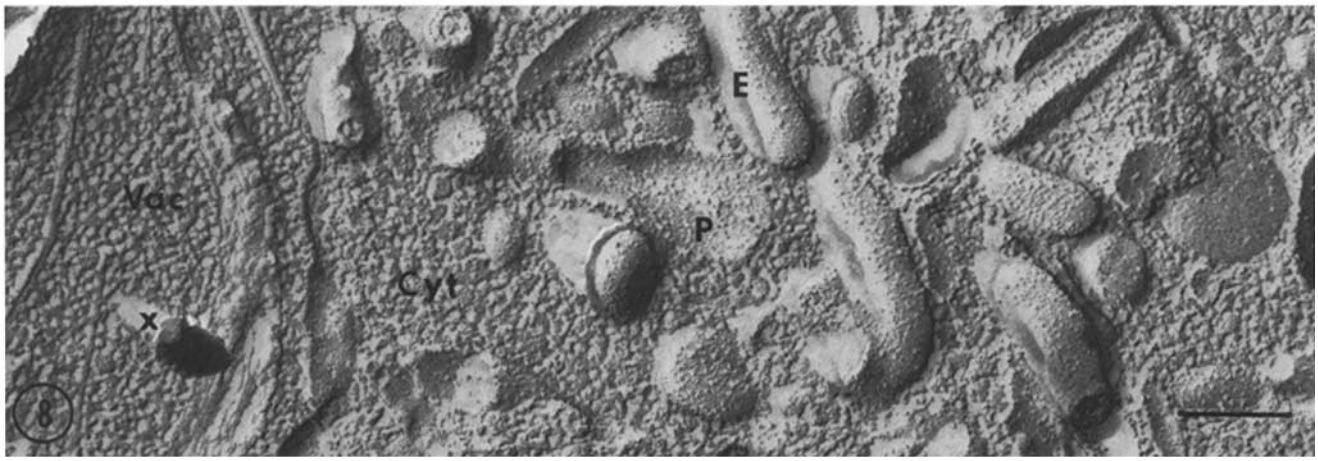
E
Vac
P
Cyt
x
8

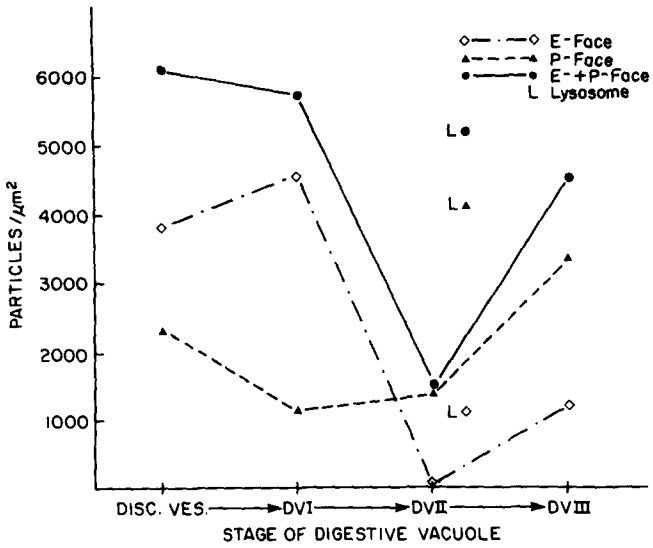

FIGURE 9 Numbers of IMPs/μm^2 on both E- and P-fracture faces of five pools of membrane of the digestive vacuole membrane system. The total number is also represented. On this basis the discoidal vesicles resemble the DV-I membranes while the DV-III membranes resemble lysosomes. DV-II membranes are dramatically different.

being distributed randomly (Fig. 16). A coating on the luminal surface of the vacuoles in this stage can sometimes be detected in freeze-fracture replicas (Fig. 17). This coating probably corresponds to the glycocalyx and paracrystalline material that has been described from thin sections (12).

Membrane Fracture Faces of Lysosomes

The elongated lysosomes (0.4 × 0.25 μm) that surround DV-II (Fig. 10) and, to a lesser extent, DV-III, and that are sometimes found to be continuous with DV-III have IMP numbers of 1,074 ± 164/μm^2 on the E face (Fig. 10, *inset*) and 4,080 ± 738/μm^2 on the P face, for a total of 5,154/μm^2 of membrane surface area. These densities are very similar to those of the DV-III. Not only are the densities of particles on the corresponding faces similar, but the particles on the E face show the same prominence as those on the E face of DV-III (Fig. 14).

Membrane Fracture Faces of Discoidal Vesicles

Discoidal vesicles have more IMPs on their E face than P face (Fig. 18) and in this way they resemble DV-I. The particle numbers are 3,810 ± 427/μm^2 for the E face, and 2,323 ± 161/μm^2 for the P face, totaling 6,133/μm^2 of membrane surface area.

IMP Size Distribution on P and E Faces

The diameters of the IMP were measured for representative areas of each membrane. Histograms of these measurements (Fig. 19) gave somewhat unexpected results. From the prominence of the IMP in the DV-III E face and on the E face of lysosomes, it seemed probable that these faces would contain a large proportion of relatively large particles. This does not seem to be the case. In fact, no large differences were seen in the size distribution of IMPs in the four populations of E faces measured (DV-I, DV-III, discoidal vesicles, and lysosomes). The major peak in all E faces was at 11 nm. Minor peaks occurred at 9, 13, and 15 nm. A small peak at 17.5 nm may be accounted for by particles composed of multiple subunits.

On the P faces there was more variability. The major peak for discoidal vesicles, lysosomes, and DV-I was 11 nm as on the E faces. Minor peaks at 8–9, 13, and 15 nm were also similar to those of the E faces. However, in DV-II and DV-III the major peak has shifted to 8.5 nm with a second peak almost equal in height at 10–10.5 nm. Smaller peaks occur at 12–12.5 and 15 nm. There is a definite increase in the percentage of IMPs of smaller diameter on the P face of DV-II and DV-III membranes.

DISCUSSION

Correlation with Other Freeze-fracture Studies

Changes in the phagosome IMP content of several different cell types have been investigated with the freeze-fracture technique. In all but one of these, the phagosome membrane differs in some way from the phagolysosome membrane. In *Acanthamoeba* the number of IMP in the initial phagosome is the same as in the plasma membrane from which it arises (10) with about two times as many IMP on the P face as the E face. Later (15 min) the number of both P- and E-face particles increases fourfold. In *Tetrahymena pyriformis*, a ciliate, the phagosomal membrane arises from the cytopharynx membrane and not directly from the plasma membrane. Thus, the nascent phagosome membrane does not resemble the plasma membrane in IMP numbers (9). Later (within 1–4 min after vacuole release into the cytoplasm) the number of IMPs doubles (13) with most of the increase occurring on the P face. In rabbit polymorphonuclear leukocytes the phagosome membranes are reported to change very little in IMP number or distribution from the plasma membrane from which they are derived (16). The P face continues to have two times as many IMPs as the E face.

Paramecium exhibits a more profound change in phagosome-phagolysosome IMP number and distribution than any of the other examples listed. However, the starting membrane from which the phagosome is derived, the cytopharynx, has a very dense population of IMPs especially on the E face (4,574 ± 733/μm^2). This membrane face then undergoes a remarkable reduction in particles over the short span of 3 min so that only 60 ± 44 IMPs/μm^2 remain. Later, as lysosomes fuse with the phagosome, the IMP density on the E face increases to 1,144 ± 338/μm^2. Whether these changes are similar to those occurring in *Tetrahymena* or *Acanthamoeba* is not clear. The initial changes occurring in *Paramecium* appear to be in the reverse direction from those in *Tetrahymena* and *Acanthamoeba*. However, since the membrane from which phagosomes are derived has a much higher population of IMPs than have these other cells, a direct comparison would be invalid. Once this load of IMPs has been removed in DV-II there is a later increase in IMPs. This increase may be comparable to that reported in the other protozoa. In no case is the significance of the IMP increase or decrease understood.

Membrane Economy during Formation and Condensation of Digestive Vacuoles

Previous observations have shown that membranes of digestive vacuoles of *Paramecium* pass through a cycle of topographical changes. Mast (14) carried out an extensive study of digestive vacuoles including the size changes of vacuoles from their time of formation until defecation. In a "typical" cycle in *P. caudatum*, the digestive vacuole or phagosome is reportedly 15 μm in diameter when first released from the oral region, but

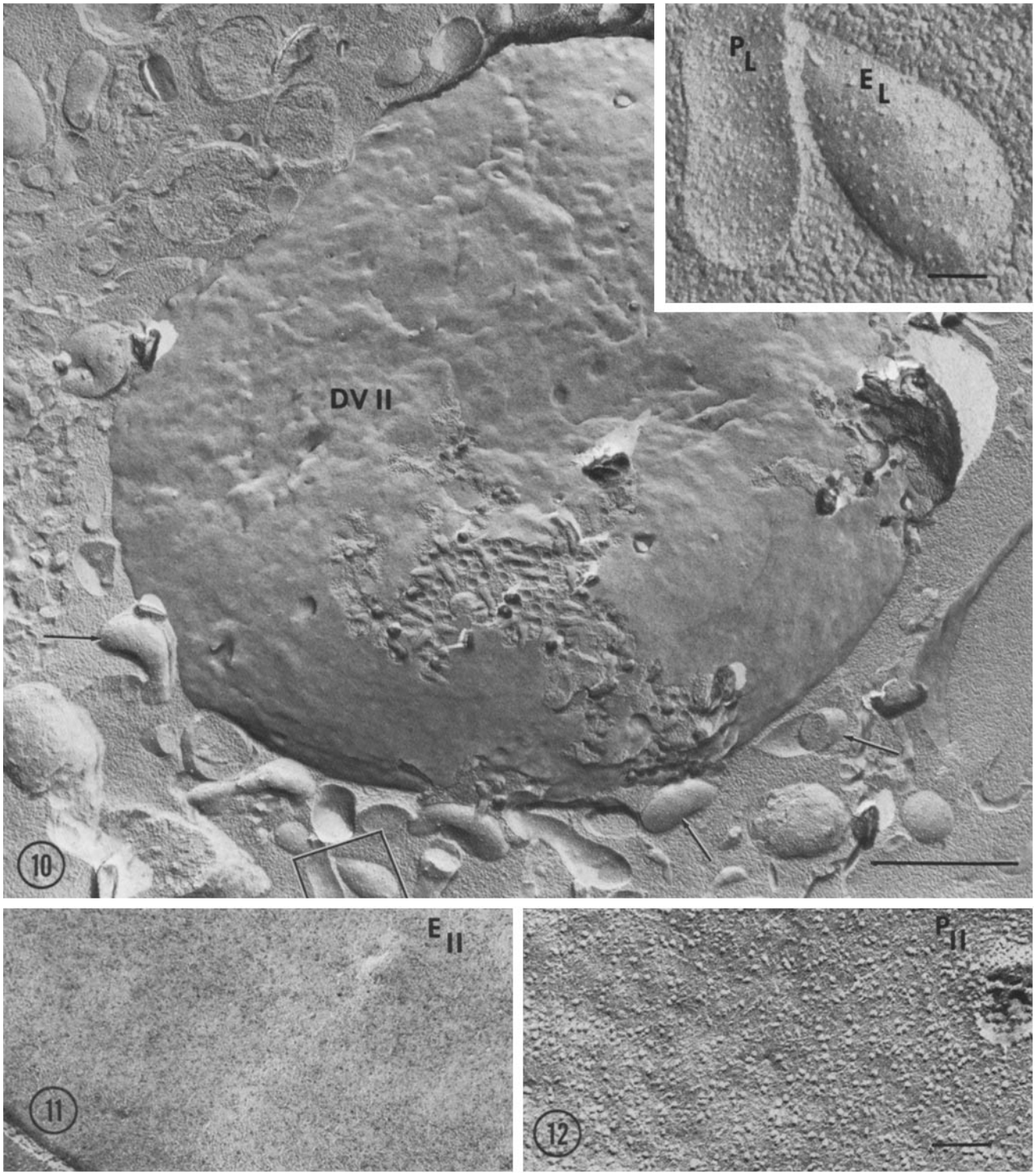

FIGURE 10 DV-II are condensed around their packed contents (fusiform structures result from stretched latex beads) and have a relatively smooth topography showing little or no endocytic activity. They are typically surrounded with lysosomes (arrows). This vacuole was 10–13 min old. The *inset* shows the P and E faces of the lysosomes enclosed by the box. Bar, 1 μm; *inset*, 0.1 μm. × 25,000; *inset*, × 100,000.

FIGURE 11 The E face of DV-II is almost devoid of IMPs. × 100,000.

FIGURE 12 The P face of DV-II contains 1,402 ± 203 IMPs/μm^2. Bar, 0.1 μm. × 100,000.

within 7 min it decreases in diameter to 6 μm. After this, the vacuole again grows in size to nearly the same diameter as it was initially.

Our timed studies of freeze-fractured vacuoles support and extend these observations of the light microscopists. The largest vacuole in our freeze-fractured replicas <3 min old was 14 μm in diameter. This was close to the diameter of the largest vacuole, 12.7 μm, in a serially thin-sectioned *P. caudatum* cell

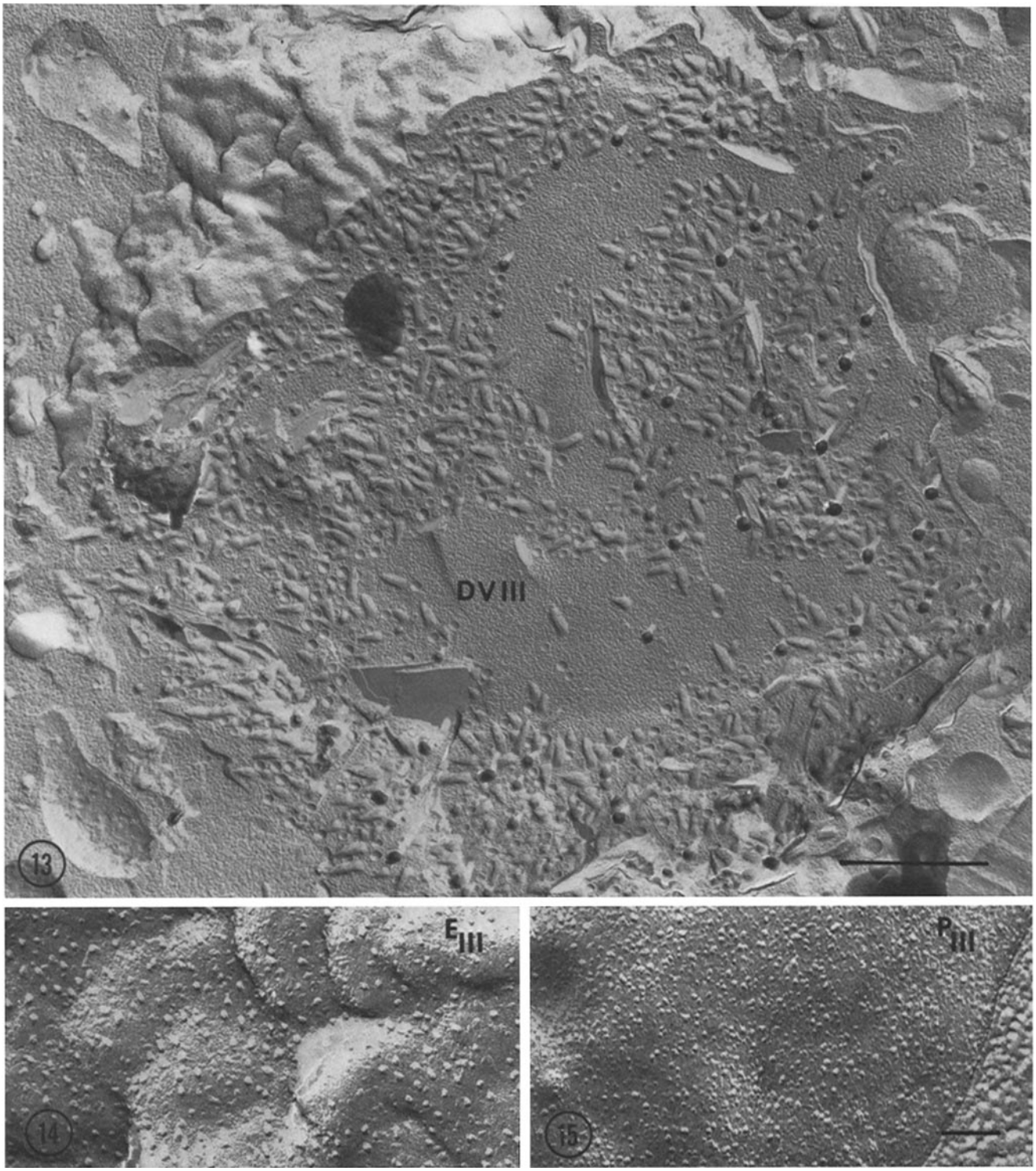

FIGURE 13 A DV-III of 32–35 min in age. The topography of the vacuole is no longer spherical but is now wavy and the diameter is much larger. The latex spheres, many deformed during fracturing, are not so tightly packed as in DV-II. Bar, 1 μm. × 25,000.

FIGURE 14 The E face of DV-III now has a population of very prominent IMPs but the total number is less than on DV-I, 1,114 ± 338/μm². × 100,000.

FIGURE 15 The P face of DV-III vacuoles has a heterogeneous population of IMPs in a much higher density than the P face of DV-I or DV-II, 3,367 ± 508/μm². Bar, 0.1 μm. × 100,000.

in which the vacuole was lying next to the oral region (unpublished observation). Vacuoles <3 min old show a high degree of blebbing along their margins. Cytosol-directed protrusions appear to result in the production of a large number of vesicles having a cylindrical shape with a diameter ~0.1 μm and a length of 0.4–0.8 μm, as well as some larger spherical blebs. On the other hand, the smaller blebs observed extending into the vacuole lumen apparently do not pinch off, but eventually

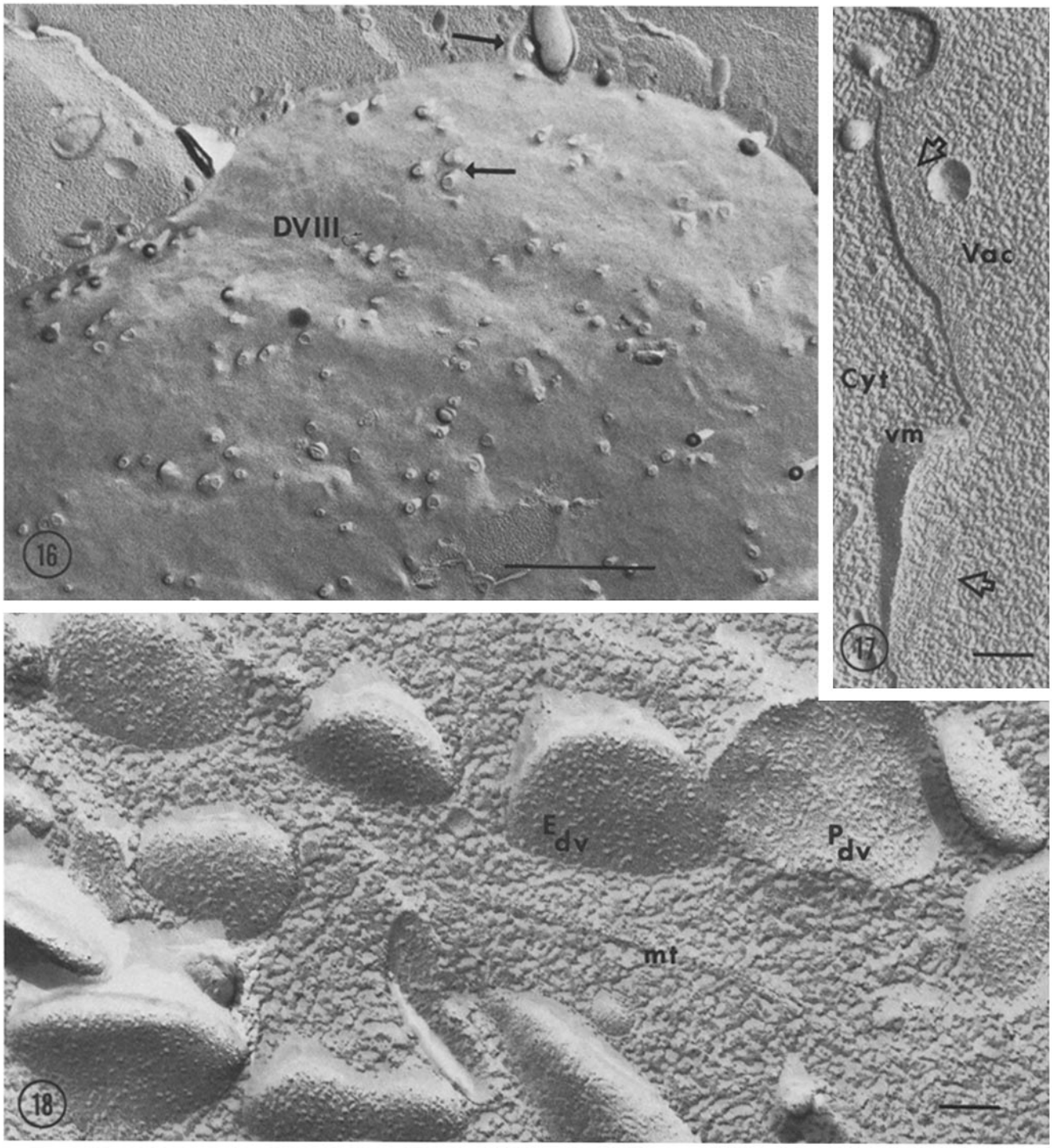

FIGURE 16 Blebbing (arrows) from a DV-III. The fractured necks appear on this E face to be grouped mostly into clumps of three to five rather than randomly scattered over the membrane surface. Bar, 1 μm. × 25,000.

FIGURE 17 A DV-III membrane (*vm*) showing continuity with a small bleb. A layer of material (arrows) distinguishable from the bulk contents of the vacuole lines the luminal surface of this vacuole membrane. *Cyt*, cytosol; *Vac*, vacuole. Bar, 0.2 μm. × 50,000.

FIGURE 18 Discoidal vesicles near the cytopharynx. Their uniformly flattened and circular profiles are evident. The P face (P_{dv}) has 2,323 ± 161 IMPs/μm^2 and the E face (E_{dv}) has 3,810 ± 427/μm^2. This membrane resembles DV-I more closely than DV-II or DV-III. *mt*, microtubular ribbon. Bar, 0.1 μm. × 100,000.

flatten out again, because no accumulation of free vesicles within the vacuoles is seen. Thus, the reduction in size of a young food vacuole (DV-I to DV-II conversion) appears to result from the removal of a large percentage of its membrane by an endocytic-like process. The ultimate amount of reduction is at least partially a function of the number of phagocytosed particles trapped within the lumen of the vacuole.

The smallest vacuole observed in freeze-fracture replicas which could be determined with reasonable certainty to be fractured through its center was 3.5 μm in diameter. The surface

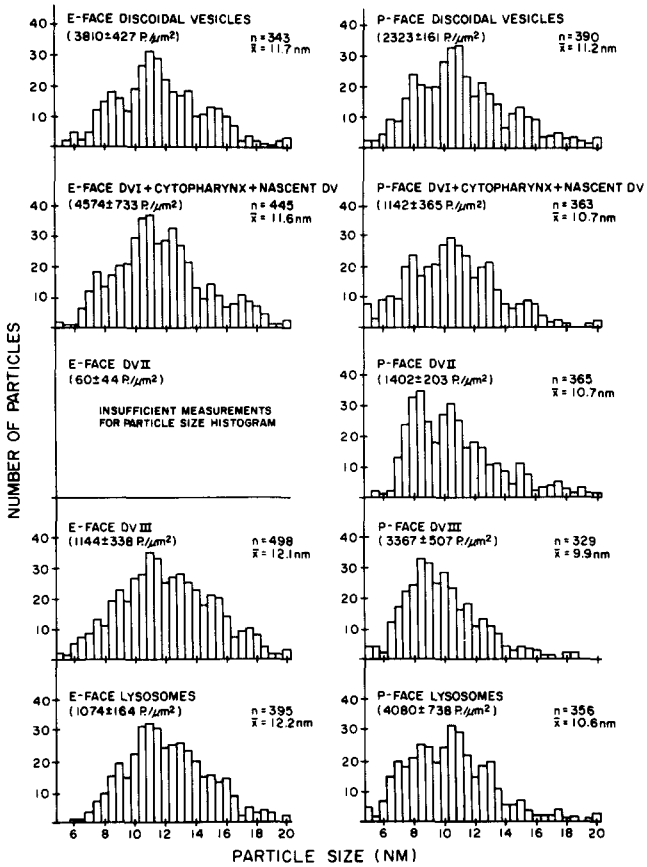

FIGURE 19 Histograms of IMP size distribution.

area of such a spherical vacuole is 38 μm^2 and its volume is 22 μm^3. Comparing this with the surface area of 616 μm^2 and volume of 1,437 μm^3 of a 14-μm-diameter DV-I, it is obvious that most of the membrane, as much as 94%, is removed during the condensation process (see Fig. 20), and the volume has been reduced an even greater extent to 1.5% of the original volume. This must be an extreme example, but it illustrates the very large amount of both membrane and vacuole fluid that can be removed during the initial short condensation phase.

Assuming an average diameter of 0.1 μm and length of 0.5 μm for the dimensions of the endosomes removed from the DV-I vacuoles, the surface area of each of these cylinders is 0.16 μm^2 and their volume is 0.0039 μm^3. The number of endosomes of these dimensions required to remove 578 μm^2 (616 minus 38) of membrane would be 3,613 (Fig. 20). The total volume of this number of endosomes, assuming that they are always removed as cylindrical vesicles, is only 14.1 μm^3. Therefore, 1,401 μm^3 of the total reduction of 1,415 μm^3 (1,437 minus 22) of volume has to be lost by other means. The active removal of membrane from the vacuole may produce a pressure on the contents of the vacuole, thereby forcing the water through the stressed (and leaky?) membrane into the cytoplasm. The very large number of IMPs in the membrane of the DV-I vacuoles may provide the polar channels through which water can rapidly pass into the cytoplasm, but at present we have no experimental evidence to support this idea. If water is selectively removed through the membrane, the increasing osmolarity of the vacuolar fluid would also produce an osmotic pressure on DV-II membranes. The observed spherical appearance of the DV-II vacuoles suggests that their contents are indeed under some physical pressure which could be caused

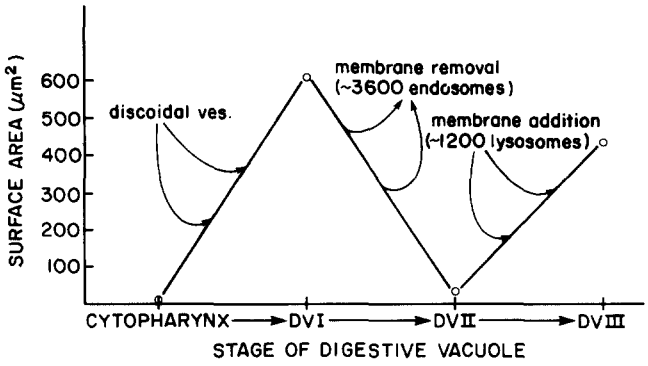

FIGURE 20 Graph denoting changes in the amount of membrane surface area as digestive vacuoles form and cycle through the cytoplasm.

by either an osmotic pressure, the rapid removal of membrane-delimited vesicles from their surface, or by a combination of both factors.

Membrane Economy during the Transition from DV-II to DV-III

Our freeze-fracture studies support the observations of Mast (14), indicating that after their condensation (DV-I to DV-II transition), the digestive vacuoles of *Paramecium* rapidly expand in size again (DV-II to DV-III transition). Re-expanded DV-III can most readily be distinguished from DV-I and DV-II by their characteristic E-face particles that resemble those seen on surrounding lysosomes (Fig. 10). For this and other reasons mentioned earlier, we propose that the expansion in the vacuoles is brought about by the fusion of DV-II vacuoles with lysosomes and the incorporation of the lysosomal membrane into the vacuole membrane.

Mast (14) reported that the expanded vacuoles reach nearly the same size as the newly formed digestive vacuoles. One fractured vacuole that appeared to have lysosomes fusing with it was 11.8 μm in diameter. It is not possible to accurately determine the surface area of these vacuoles because of their irregular topography, but if this vacuole were spherical it would have a surface area of 437 μm^2 and a volume of 860 μm^3. To increase the membrane area from 38 to 437 μm^2, from DV-II to DV-III, would require the addition of 399 μm^2 of membrane (Fig. 20). A typical lysosome has a shape approximating a prolate spheroid with a major axis of 0.428 μm and a minor axis of 0.228 μm. Its surface area is 0.33 μm^2 and its volume is 0.116 μm^3. Thus at least 1,209 lysosomes would be required to fuse with the DV-II vacuole to increase its surface area to that of a DV-III vacuole of the size given above. The volume contained by this number of lysosomes only equals 14 μm^3. Therefore, most of the volume increase in these vacuoles must result from the return of water and diffusible molecules from the cytoplasm into the vacuole.

These calculations lead to a consideration of the function of such a tremendous shrinking and swelling of vacuoles. Possibly, the cell needs to concentrate its food before digestion to allow for more efficient utilization of the hydrolytic enzymes. However, the food would be diluted again to approximately the same extent after expansion. Another possibility, which may be just as important to the cell, is that membrane material needs to be recovered (lipids and surface receptors) for recycling back to the cytopharynx to allow rapid digestive vacuole formation, a type of selective removal of specific membrane

components as occurs in fibroblasts (19). In line with this, to account for the significant loss of IMPs from the vacuole membrane remaining during the DV-I to DV-II transition, one could postulate that the endosomes remove selectively and proportionately more particles than lipids.

The condensation of the vacuole may also contribute indirectly to the killing of the food organisms. Mast (14) reported that bacteria stop moving in the condensed vacuoles. Concentrating the initial volume of materials not capable of passing through the membrane into a much smaller volume will certainly drastically affect the concentration of such substances. In terms of inactivation of food organisms, a sudden increase in protons (lower pH) and of salts could produce a toxic effect.

Membrane Economy in Actively Digesting Vacuoles

According to Mast (14) digestion does not begin until the vacuoles begin to expand. This too seems to be confirmed by our study. Lysosomes do not appear to fuse with phagosomes, as judged by the appearance of IMPs characteristic of lysosomes in the DV-III membranes (Figs. 10 and 14), until the onset of vacuole expansion, membrane expansion being a consequence of this fusion. Because partially digested organisms do not appear in fractured vacuoles before this stage, the DV-II to DV-III transition seems to coincide with the phagosome to phagolysosome transition of these organelles.

We have not observed any noticeable change in IMP numbers or distribution in DV-III after they have completed their expansion. However, evidence of budding activity is a more or less constant feature of these vacuoles. We suspect that secondary "lysosomes," with or without hydrolases, may be removed from the vacuoles during this stage.

This study has not examined vacuoles at defecation because this event is rarely encountered and cannot be pulsed for freeze-fracture study. We know from conventional thin-sectioning that the digestive vacuole membrane is re-engulfed at the cell anus (cytoproct) by endocytosis (8) and the initial endosomes are tubular (2, 8). As recently shown in a cytochemical study by Allen and Fok (7), the endosomes formed at the cytoproct are transformed into discoidal vesicles and then passed along microtubular ribbons back to the oral region for reuse in digestive vacuole formation. The present study indicates that besides the discoidal vesicles that arise at the cytoproct, other vesicles are formed in very large numbers from condensing DV-I or even DV-III which conceivably could be used in vacuole formation. The fates of vesicles arising from DV-I and DV-III are currently under investigation.

Implications of Changes in IMP Number and Distribution with Vacuole Age

Fig. 9 displays the numbers of particles in a 1-μm^2 surface area as given in Fig. 19 for each of five different stages in the digestive vacuole membrane system. Totals for the E faces, P faces, and overall totals are graphed. The similarity between discoidal vesicle membranes and DV-I membranes, and between lysosome membranes and DV-III membranes is evident. The dissimilarity between DV-II vacuole membranes and either of these other four groups of membranes is also very obvious.

The appearance and disappearance of IMPs are most easily explained, as we have done, by the fission or fusion with the vacuole membrane (Fig. 21) of vesicles bearing differing IMP populations. However, other interpretations are possible. These include splitting of IMP as has been shown to be possible during membrane fracturing (11), or the dispersion and consequent disappearance within the membrane of the monomers which aggregate to form an IMP (20) or changes in the fracture pattern caused by altered IMP binding to structures on either surface of the vacuole membrane. However, since we are fixing and glycerinating all cells in the same way at all time periods the changes we see under the experimental procedure used reflect basic changes within the membranes themselves or with the binding properties of the IMP to external factors outside the membrane. This is not to say that we would see the identical changes if different preparative procedures were used such as rapid freezing at lower temperatures without prior fixation (for discussions of artifacts see reference 17). Corroboration of our results using techniques that approach the in vivo conditions of the cell are, of course, always desirable.

These freeze-fracture results on digestive vacuoles of known age in *P. caudatum* do not contradict the previous finding that digestive vacuole membrane is derived from a pool of discoidal vesicles (Fig. 21) (1), some of which arise from recycled defecation vacuole membrane (7). What the present study has shown is that the membranes of nascent phagosomes and discoidal vesicles are similar in all of the IMP parameters (density, size, and fracture-face distribution) and that the condensation of DV-I to DV-II is such that up to 90% of the initial DV-I membrane is retrieved in a very specific manner for possible direct recycling to the cytopharynx membrane. In this context it is interesting to note that the surface area of the DV-I-derived endosomes is very similar to the surface area of the discoidal vesicles, but further studies are needed to clarify this relationship. Our particle size and density measurements suggest that the protein composition of the DV-II membrane is very different from the composition of the DV-I and DV-III membranes. However, the fusion of lysosomes with the DV-II vacuole produces DV-III vacuoles with membranes resembling lysosomes in their IMP parameters. This is not all that unexpected when one considers that close to 90% of the final DV-III membrane may be lysosome-derived. Although blebbing occurs from DV-III vacuoles, its extent, significance, and effect on the IMP parameters are not known.

The principal contribution of this study is the demonstration that membranes are differentiated in parallel with the process of phagocytosis and intracellular digestion. At present we are not certain, at the molecular or physiological levels, what these changes mean or what the function is of the digestive vacuole IMPs. However, on the basis of studies of other membrane

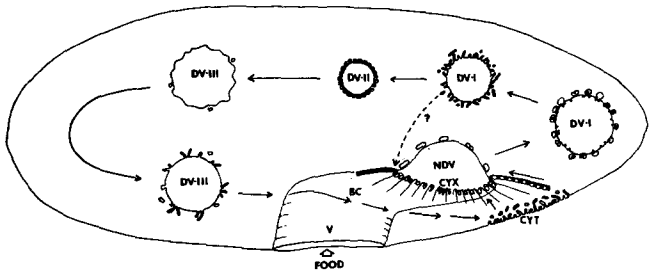

FIGURE 21 A diagram of *P. caudatum* illustrating membrane events at the surface of digestive vacuoles and possible membrane flow patterns in the digestive system. Question mark indicates path that is not yet certain. *BC*, buccal cavity; *CYT*, cytoproct; *CYX*, cytopharynx; *NDV*, nascent digestive vauole; *V*, vestibulum.

systems (15, 20, 21), we may assume that they represent structural equivalents of intramembrane protein complexes. Our ultimate goal will be to determine what the IMP functions are and how the changes in membrane structure relate to the physiological processes occurring within the vacuoles.

The invaluable instruction on the Balzers given R. D. Allen by Stephanie Krah is gratefully acknowledged, as are the useful discussions with Dr. A. K. Fok.

The research was supported by National Institutes of Health grants GM-17991 to R. D. Allen and GM 18639 to L. A. Staehelin, and National Science Foundation grant PCM 78-15893 to R. D. Allen.

Received for publication 21 July 1980, and in revised form 3 December 1980.

REFERENCES

1. Allen, Richard D. 1974. Food vacuole membrane growth with microtubule-associated membrane transport in *Paramecium*. *J. Cell Biol.* 63:904–922.
2. Allen, Richard D. 1976. Freeze-fracture evidence for intramembrane changes accompanying membrane recycling in *Paramecium*. *Cytobiologie.* 23:254–273.
3. Allen, Richard D. 1976. Membranes of digestive vacuoles: Topography and intramembrane particle changes with time. *J. Cell Biol.* 70(2, Pt. 2):386 *a* (Abstr.).
4. Allen, Richard D. 1977. Intramembrane alterations that occur in digestive vacuoles of *Paramecium*. *In* 4th International Congress on Protozoology. S. H. Hutner, editor. Abstr. 235.
5. Allen, Richard D. 1978. Particle arrays in the surface membrane of *Paramecium*: Junctional and possible sensory sites. *J. Ultrastruct. Res.* 63:64–78.
6. Allen, Richard D. 1978. Membranes of ciliates: Ultrastructure, biochemistry and fusion. *In* Membrane Fusion, G. Poste and G. L. Nicolson, editors. Elsevier/North-Holland Biomedical Press, Amsterdam. 657–763.
7. Allen, Richard D., and A. K. Fok. 1980. Membrane recycling and endocytosis in *Paramecium* confirmed by horseradish peroxidase pulse-chase studies. *J. Cell Sci.* 45:131–145.
8. Allen, Richard D., and R. W. Wolf. 1974. The cytoproct of *Paramecium caudatum*: structure and function, microtubules, and fate of food vacuole membranes. *J. Cell Sci.* 14: 611–631.
9. Batz, W., and F. Wunderlich. 1976. Structural transformation of the phagosomal membrane in *Tetrahymena* cells endocytosing latex beads. *Arch. Microbiol.* 109:215–220.
10. Bowers, B. 1980. A morphological study of plasma and phagosome membranes during endocytosis in *Acanthamoeba*. *J. Cell Biol.* 84:246–260.
11. Edwards, H. H., T. J. Mueller, and M. Morrison. 1979. Distribution of transmembrane polypeptides in freeze fracture. *Science (Wash. D. C.).* 203:1343–1346.
12. Fok, A. K., and Richard D. Allen. 1979. Axenic *Paramecium caudatum*. I. Mass culture and morphology. *J. Protozool.* 26:463–470.
13. Kitajima, Y., and G. A. Thompson, Jr. 1977. Differentiation of food vacuolar membranes during endocytosis in *Tetrahymena*. *J. Cell Biol.* 75:436–445.
14. Mast, S. O. 1947. The food-vacuole in *Paramecium*. *Biol. Bull.* 92:31–72.
15. McDonnel, A., and L. A. Staehelin. 1980. Adhesion between lysosomes mediated by the chlorophyll a/b light-harvesting complex isolated from chloroplast membranes. *J. Cell Biol.* 84:40–56.
16. Moore, P. L., H. L. Bank, N. T. Brissie, and S. S. Spicer. 1978. Phagocytosis of bacteria by polymorphonuclear leukocytes. A freeze-fracture, scanning electron microscope, and thin-section investigation of membrane structure. *J. Cell Biol.* 76:158–174.
17. Rash, J. E., and C. S. Hudson, editors. 1979. Freeze Fracture: Methods, Artifacts, and Interpretations. Raven Press, New York.
18. Rosenbaum, R. M., and M. Wittner. 1962. The activity of intracytoplasmic enzymes associated with feeding and digestion in *Paramecium caudatum*. The possible relationship to neutral red granules. *Arch. Protistenk.* 106:223–240.
19. Schneider, Y. J., P. Tulkens, C. de Duve, and A. Trouet. 1979. Fate of plasma membrane during endocytosis. II. Evidence for recycling (shuttle) of plasma membrane constituents. *J. Cell Biol.* 82:466–474.
20. Segrest, J. P., T. Gulik-Krzywicki, and C. Sardet. 1974. Association of the membrane-penetrating polypeptide segment of the human erythrocyte MN-glycoprotein with phospholipid bilayers. I. Formation of freeze-etch intramembranous particles. *Proc. Natl. Acad. Sci. U. S. A.* 71:3294–3298.
21. Skriver, E., A. B. Maunsbach, and P. L. Jørgensen. 1980. Ultrastructure of Na, K-transport vesicles reconstituted with purified renal Na, K-ATPase. *J. Cell Biol.* 86:746–754.
22. Staehelin, L. A. 1976. Reversible particle movements associated with unstacking and restacking of chloroplast membranes in vitro. *J. Cell Biol.* 71:136–158.
23. Willison, J. H. M., B. W. W. Grout, and E. C. Cocking. 1971. A mechanism for the pinocytosis of latex spheres by tomato fruit protoplasts. *Bioenergetics.* 2:371–382.